IAI Journals.ASM.org

Site-Dependent Recruitment of Inflammatory Cells Determines the Effective Dose of *Leishmania major*

Flavia L. Ribeiro-Gomes,[a]* Eric Henrique Roma,[a,b] Matheus B. H. Carneiro,[a,b] Nicole A. Doria,[a] David L. Sacks,[a] Nathan C. Peters[a]

Laboratory of Parasitic Diseases, National Institute of Allergy and Infectious Diseases, National Institutes of Health, Bethesda, Maryland, USA[a]; Laboratório de Gnotobiologia e Imunologia, Departamento de Bioquímica e Imunologia, Instituto de Ciências Biológicas, Universidade Federal de Minas Gerais, Belo Horizonte, Minas Gerais, Brazil[b]

The route of pathogen inoculation by needle has been shown to influence the outcome of infection. Employing needle inoculation of the obligately intracellular parasite *Leishmania major*, which is transmitted in nature following intradermal (i.d.) deposition of parasites by the bite of an infected sand fly, we identified differences in the preexisting and acute cellular responses in mice following i.d. inoculation of the ear, subcutaneous (s.c.) inoculation of the footpad, or inoculation of the peritoneal cavity (intraperitoneal [i.p.] inoculation). Initiation of infection at different sites was associated with different phagocytic populations. Neutrophils were the dominant infected cells following i.d., but not s.c. or i.p., inoculation. Inoculation of the ear dermis resulted in higher frequencies of total and infected neutrophils than inoculation of the footpad, and these higher frequencies were associated with a 10-fold increase in early parasite loads. Following inoculation of the ear in the absence of neutrophils, parasite phagocytosis by other cell types did not increase, and fewer parasites were able to establish infection. The frequency of infected neutrophils within the total infected CD11b$^+$ population was higher than the frequency of total neutrophils within the total CD11b$^+$ population, demonstrating that neutrophils are overrepresented as a proportion of infected cells. Employing i.d. inoculation to model sand fly transmission of parasites has significant consequences for infection outcome relative to that of s.c. or i.p. inoculation, including the phenotype of infected cells and the number of parasites that establish infection. Vector-borne infections initiated in the dermis likely involve adaptations to this unique microenvironment. Bypassing or altering this initial step has significant consequences for infection.

The route or site of inoculation has been shown to significantly influence disease outcome in numerous models of infection, including *Leishmania* (1–9), *Toxoplasma* (10), *Plasmodium* (11), *Listeria* (12–14), *Borrelia* (15), and influenza virus (16, 17) infections. Vaccination by different routes has also been shown to influence the efficacy of vaccines against parasitic, bacterial, and viral infections, as well as cancer (3, 18–28). In the case of infections initiated in the skin by the bite of an insect vector, such as *Yersinia*, *Plasmodium*, *Borrelia*, and *Leishmania* infections (29), the use of an intradermal route of infection would appear to be critical, since the initial interaction between these pathogens and the host takes place primarily in the skin under natural conditions (11, 15, 30–32). However, the factors that determine site- or route-specific influences on infection or vaccination remain poorly defined.

Following infection with intracellular pathogens such as *Leishmania*, the degree to which different phagocytic cells take up the organism and are permissive to its long-term intracellular survival and growth will significantly influence the outcome of infection. In nature, *Leishmania* infection is established following exposure of the skin to the bites of an infected phlebotomine sand fly. Infected sand fly bite sites are characterized by the deposition of parasites throughout the dermal and epidermal layers of the skin and by robust and sustained recruitment of neutrophils. Neutrophils also represent the majority of infected cells early after sand fly or intradermal (i.d.) needle inoculation of *Leishmania major* (33, 34). *L. major* parasites remain viable following phagocytosis by neutrophils, and neutrophil depletion prior to transmission by sand fly bite compromises the establishment of infection. While it may seem obvious that i.d. needle inoculation of the skin would best replicate both the anatomical placement of parasites and the associated recruitment of inflammatory cells observed following the bite of an infected sand fly, subcutaneous (s.c.) inoculation of the footpad (f.p.) remains a favored route of infection, and more recently, intraperitoneal (i.p.) inoculation has been used to emphasize the importance of rapidly recruited inflammatory monocytes in *Leishmania* infection (35). A careful study of the preexisting and recruited populations of phagocytic cells at different sites of needle inoculation and the potential impact of these cells on acute-infection outcome has not been done. Here we find that the initiation of *L. major* infection by i.d. inoculation of the ear, compared to s.c. inoculation of the footpad or inoculation via the i.p. route, is associated with the presence of different phagocytic cell types, especially neutrophils, and that this correlates with a much greater total number of infected cells at early time points postinfection (p.i.). These observations provide strong evidence that attempts at reproducing the natural site of inoculation are consequential, impacting subsequent parasite loads and infected-cell phenotypes.

Received 13 December 2013 **Returned for modification** 19 January 2014
Accepted 30 March 2014
Published ahead of print 14 April 2014
Editor: J. A. Appleton
Address correspondence to Nathan C. Peters, NPeters@niaid.nih.gov.
* Present address: Flavia L. Ribeiro-Gomes, Federal University of Rio de Janeiro, Rio de Janeiro, Brazil.
F.L.R.-G. and E.H.R. contributed equally to this article.

doi:10.1128/IAI.01600-13

MATERIALS AND METHODS

Mice. Female C57BL/6 mice were purchased from Taconic Farms. Mice were 6 to 10 weeks of age. All mice were maintained in the National Institute of Allergy and Infectious Diseases animal care facility under specific-pathogen-free conditions.

Parasite preparation and needle inoculation. The *L. major* NIH Friedlin V1 (FV1) strain was originally obtained from the Jordan Valley (MHOM/IL/80/FN). A stable transfected line of *L. major* FV1 promastigotes expressing a red fluorescent protein (*L. major*-RFP) was generated as described previously (36). Parasites were grown *in vitro* at 26°C in medium 199 supplemented with 20% heat-inactivated fetal calf serum (FCS; Gemini Bio-Products), 100 U/ml penicillin, 100 μg/ml streptomycin, 2 mM L-glutamine, 40 mM HEPES, 0.1 mM adenine (in 50 mM HEPES), 5 mg/ml hemin (in 50% triethanolamine), and 1 mg/ml biotin. *L. major*-RFP was grown in the presence of 50 μg/ml Geneticin (G418; Sigma). Infective-stage metacyclic promastigotes were isolated from stationary-phase cultures (4 to 5 days old) by negative selection of infective forms using peanut agglutinin (PNA; Vector Laboratories Inc., Burlingame, CA) (37). Mice were infected either (i) in the ear dermis by intradermal (i.d.) injection using a 29 1/2-gauge, 3/10-ml insulin syringe (BD Biosciences) in a volume of 10 μl, (ii) in the footpad (f.p.) by subcutaneous (s.c.) injection using the same 29 1/2-gauge, 3/10-ml insulin syringe in a volume of 40 μl, or (iii) in the peritoneal cavity (intraperitoneal [i.p.] inoculation) using a 27-gauge, 1-ml syringe in a volume of 200 μl. Care was taken during footpad injections to avoid the intramuscular and/or intradermal tissue. The dose of parasites and the timing of analysis are specified below.

Exposure of mice to the bites of uninfected sand flies. Mice were anesthetized by intraperitoneal injection of 30 μl of ketamine-xylazine (100 mg/ml). Mice were placed in a 1-cubic-foot Plexiglas container with approximately 1,500 female *Phlebotomus duboscqi* sand flies. The tail, eyes, nose, and front paws were covered to encourage feeding on the ears and hind footpads. Sand flies were allowed to feed at will for 90 to 120 min.

Preparation of cells from different anatomical locations. Prior to or following *Leishmania* inoculation, mice were euthanized and perfused; the ears or footpads were removed; and mice were placed in 70% ethanol for 2 to 5 min. Separated dorsal and ventral sheets of ears or total footpad tissue following removal of the toes and bones were incubated at 37°C for 90 min in 1 ml Dulbecco's modified Eagle medium (DMEM) containing 160 μg/ml of Liberase TL purified enzyme blend (Roche Diagnostic Corp.). Following Liberase treatment, the tissue was homogenized for 3 1/2 min in a Medicon instrument (Becton Dickinson). The tissue homogenate was then flushed from the Medicon instrument with 10 ml RPMI medium containing 0.05% DNase and was filtered using a 50-μm-pore-size cell strainer. For the preparation of cells for cell surface staining, the tissue homogenate was spun down for 10 min at 1,500 rpm and was resuspended in the appropriate medium. Peritoneal cells were harvested by flushing the peritoneal cavity with 5 ml DMEM, washed, and resuspended in the appropriate medium.

Phenotypic analysis of cell populations. Cells derived from ears, footpads, or peritoneal cavities were incubated with an antibody (Ab) against the Fc-γ III/II (CD16/32) receptor (2.4G2; BD Biosciences) in RPMI medium without phenol red (Gibco) and containing 1.0% FCS for 10 min, followed by incubation for 20 min with a combination of five or seven of the following antibodies: phycoerythrin (PE)-Cy7- or V450-conjugated anti-CD11b (M1/70), peridinin chlorophyll protein (Per-CP) Cy5.5-conjugated anti-Ly6C (HK1.4), fluorescein isothiocyanate (FITC)- or PE-conjugated anti-Ly6G (1A8), Per-CP Cy5.5-, V450-, or PE-Cy7-conjugated anti-CD11c (HL3), allophycocyanin (APC)-, V450-, or APC-Cy7-conjugated anti-F4/80 (BM8), Alexa Fluor 700- or APC-conjugated anti-mouse major histocompatibility complex class II (MHC-II) (M5/114.15.2), and FITC-conjugated anti-Gr-1 (RB6-8C5). The isotype controls employed were rat IgG1 (R3-34) and rat IgG2b (A95-1 or eBR2a). Data were collected using FACSDiva software on a FACSCanto flow cytometer (BD Biosciences) and were analyzed using FlowJo software (TreeStar).

Restimulation of tissue-derived cells for cytokine analysis by flow cytometry. T cells were restimulated with parasite antigen as described previously (38). Briefly, whole-ear single-cell suspensions were incubated at 37°C under 5% CO_2 for 12 to 14 h in flat-bottom 48-well plates with 1×10^6 T cell-depleted (Miltenyi Biotech), irradiated naïve spleen cells (antigen-presenting cells), with or without 50 μg/ml freeze-thawed *Leishmania* antigen (*L. major*-Ag). During the final 4 h of culture, 1 μg/ml of brefeldin A (GolgiPlug; BD Biosciences) was added. Following *in vitro* culture, washed cells were labeled with Live/Dead fixable Aqua stain (Invitrogen) to exclude dead cells and with an anti-Fc-γ III/II (CD16/32) receptor Ab (2.4G2), followed by PE-Cy7-conjugated anti-mouse CD4 (RM4-5) for 20 min. Cells were then fixed with BD Cytofix/Cytoperm (BD Biosciences) and were stained with V500-conjugated anti-CD3 (145-2C11) and an FITC-conjugated antibody against gamma interferon (IFN-γ) (XMG1.2). The isotype controls employed were rat IgG1 (R3-34) and rat IgG2b (A95-1 or eBR2a). All Abs were from eBioscience or BD Biosciences. Data were collected using FACSDiva software on a FACSCanto flow cytometer (BD Biosciences) and were analyzed with FlowJo software (TreeStar). Forward-scatter (FSC) and side-scatter (SSC) widths were employed to exclude cell doublets from analysis.

Real-time PCR. For analysis of cytokine gene expression, a proportion of ear or footpad tissue from infected or naïve mice was prepared as described above and was placed in RNAlater (Qiagen). Homogenates were then passed through QIAshredder columns, and RNA was purified by using an RNeasy minikit according to the manufacturer's protocol (Qiagen). Reverse transcription was performed using the SuperScript III first-strand synthesis system for reverse transcription-PCR (RT-PCR) (Invitrogen Life Technologies). Real-time PCR was performed on an ABI Prism 7900 sequence detection system (Applied Biosystems). Primer-probe sets were from predeveloped gene expression assays designed by Applied Biosystems. The quantity of the product was determined by the comparative threshold cycle method using $2^{-\Delta\Delta CT}$ (where C_T represents the cycle threshold) to determine the fold increase. Each gene was normalized to the 18S rRNA endogenous control, and the fold change in expression relative to naïve controls is reported.

Determination of parasite load by LDA or quantification of RFP^+ cells. For limiting dilution analysis (LDA), a proportion of the tissue homogenate from each site was spun at parasite speed (4,000 rpm), suspended in parasite growth medium, and serially diluted in 96-well flat-bottom microtiter plates, in which 100 μl was overlaid on 50 μl of Novy-MacNeal-Nicolle (NNN) medium containing 20% defibrinated rabbit blood. The number of viable parasites was determined from the highest dilution at which promastigotes could be grown after 7 to 10 days of incubation at 26°C. The number of RFP^+ cells per site was determined in the context of phenotypic analysis, as described above. In some experiments, counting beads (AccuCheck; Invitrogen) were mixed with a cell aliquot obtained following a cell speed (1,500 rpm) spin of the tissue homogenate, and the absolute number of cells per sample was determined according to the manufacturer's instructions.

Neutrophil depletion. Neutrophils were depleted by i.p. injection of antibody RB6-8C5 (anti-Gr-1), 1A8 (anti-Ly6G; BioXCell), NIMP-R14 (undefined; NIAID Custom Antibody Service Facility), or GL113 (control IgG; BioXCell) in 200 μl. The amount and timing of antibody administration are specified below.

Statistics. Data following a normal distribution were compared using Student's *t* test. For comparisons between three groups, 1-way analysis of variance (ANOVA) was performed. Data that did not follow a normal distribution were compared using the Mann-Whitney test. All *P* values are two-sided. Statistical calculations were done in GraphPad Prism, version 5.0c. Levels of significance are reported as follows, unless otherwise indicated; *, $0.05 > P > 0.005$; **, $0.005 > P > 0.0005$; ***, $P < 0.0005$. Error bars represent the standard deviations (SD) of the means unless otherwise indicated.

Ethics statement. All animal experiments were performed under an animal study protocol approved by the NIAID Animal Care and Use

Committee using guidelines established by the Animal Welfare Act and the PHS Policy on Humane Care and Use of Laboratory Animals.

RESULTS

The route of *L. major* inoculation by needle determines the initial host cell phenotype and the number of parasites that establishes infection. To determine the impact of the inoculation site on the phenotypes of preexisting and recruited phagocytic cells, C57BL/6 mice were needle inoculated in the ear (i.d.), footpad (s.c.), or peritoneal cavity (i.p.) with 1×10^6 *L. major* metacyclic promastigotes expressing a red florescent protein (*L. major*-RFP). A high dose of parasites was employed to allow for the detection of sufficient numbers of RFP^+ infected cells by flow cytometry. Phenotypic analysis of naïve mice or mice infected with *L. major*-RFP parasites 10 h previously revealed that Ly6G and F4/80 expression on $CD11b^+$ cells from the ear was similar to that from the footpad (Fig. 1A). In contrast, the peritoneal cavity contained $Ly6G^-$ populations that expressed no, intermediate, or high levels of F4/80. Ly6C and F4/80 coexpression on $CD11b^+$ cells in the peritoneal cavity following infection revealed a highly diverse population of cells, in contrast to those in the ear or footpad (Fig. 1B). $CD11b^+$ $Ly6G^-$ cells from the ear and footpad contained a well-defined population of $CD11c^+$ $MHC\text{-}II^+$ dendritic cells (DCs), whereas this population was less distinct in the peritoneal cavity (Fig. 1A, bottom). While the total number of $CD11b^+$ cells recovered from each site following infection was the same (Fig. 1C), the efficiency of cell recovery from different sites of infection may be different. Therefore, we investigated the prominence of different phagocytic cell types at each infected site as a proportion of $CD11b^+$ cells (Fig. 1D). The frequency of $Ly6G^+$ $F4/80^-$ neutrophils was dramatically higher in the ear than in the footpad or peritoneal cavity (Fig. 1D, left). In contrast, the footpad and peritoneal cavity contained much higher frequencies of $CD11b^+$ $Ly6G^-$ $F4/80^+$ $(CD11c\ MHC\text{-}II)^-$ monocytes/macrophages (Mono./Mac.) than the ear (Fig. 1D, center). In the ear, neutrophils were present at higher frequencies than Mono./Mac. (P, <0.005) or $CD11c^+$ $MHC\text{-}II^+$ DCs (P, <0.0005), while in the footpad and peritoneal cavity, Mono./Mac. were the dominant cell type, as opposed to neutrophils or DCs (P, <0.0005). Neutrophils derived from different infected sites at 2 h p.i. were also morphologically different (Fig. 1E): neutrophils from the ear were significantly smaller (SSC) and possessed higher granularity (FSC) than those from the footpad and the peritoneal cavity.

Analysis of RFP expression at each site in naïve mice, or in mice infected 10 h previously with wild-type or RFP-expressing *L. major*, allowed subsequent phenotyping of infected cells in *L. major*-RFP-infected mice (Fig. 2A and B). Despite the recovery of similar numbers of $CD11b^+$ cells from the different sites (Fig. 1C) (the mice for which results are shown in Fig. 1 and 2 are from the same experiment), the peritoneal cavity returned the largest number of $CD11b^+$ RFP^+ cells, while the footpad returned the smallest number of infected cells (Fig. 2C, left). This was also true when the frequency of RFP^+ cells among $CD11b^+$ cells was assessed (Fig. 2C, right). As we have reported previously (33), neutrophils represented the majority (75%) of $CD11b^+$ RFP^+ infected cells following i.d. inoculation of the ear (Fig. 2D, left, filled circles). Strikingly, neutrophils represented a much larger percentage of $CD11b^+$ RFP^+ infected cells in the ear (75%) than in the footpad (37%) or peritoneal cavity (16%) (Fig. 2D, left). In contrast, monocytes/macrophages represented the majority of infected cells in the footpad (52%) and peritoneal cavity (68%) (Fig. 2D, center). DCs represented only 5% of infected cells in the ear and footpad, and 10% in the peritoneal cavity (Fig. 2D, right). The abundant $CD11b^+$ $Ly6G^-$ $F4/80^-$ population unique to the peritoneal cavity remained almost completely uninfected (compare Fig. 1A and 2B). Of the large number of infected $Ly6G^-$ $F4/80^+$ cells in the peritoneal cavity, the majority (69.4% ± 11.7% [mean ± SD; $n = 6$]) were $F4/80^{high}$ $CD11b^{high}$ peritoneal macrophages (PMs) (39).

Comparison of the frequency of infected neutrophils within the total $CD11b^+$ infected population with the frequency of total neutrophils within the total $CD11b^+$ population revealed that neutrophils are overrepresented as a proportion of infected versus total $CD11b^+$ cells (Fig. 2D, filled versus open circles). In contrast, Mono./Mac. were underrepresented among infected cells, and the same was true for DCs in the ear and footpad. Therefore, neutrophils appear to be more efficient at acquiring parasites than Mono./Mac. regardless of the site of infection and more efficient than DCs in the ear and footpad. The larger number of neutrophils in the ear than in the footpad also correlated with the larger number and frequency of total infected $CD11b^+$ cells (Fig. 1C).

Kinetic analysis of infection following inoculation of the ear or footpad. Since the ear and footpad represent the most common sites employed in studies of cutaneous leishmaniasis, we investigated the early kinetics of infection at these two sites in more detail. The total numbers of $CD11b^+$ cells at each site were similar until 9 days postinfection, when more cells were found in the ear (Fig. 3A) (P, <0.001). Prior to challenge, $CD11b^+$ cells at both sites were predominantly $Ly6G^-$ $Ly6C^{negative/low}$ ($Ly6C^{neg/lo}$) (Fig. 3B and C, 0 h), suggesting a resident macrophage/DC phenotype. Following infection, the proportion of $Ly6G^-$ $Ly6C^{neg/lo}$ cells dropped significantly (P, ≤ 0.0018) in the ear (Fig. 3C, left), concurrent with a 100-fold increase in neutrophil numbers over those in naïve mice (Fig. 3D, center). A less dramatic recruitment of $Ly6G^-$ $Ly6C^{high}$ ($Ly6G^-$ $Ly6C^{hi}$) inflammatory monocytes occurred in the ear at 2 h. p.i., confirming our previous observation that neutrophil recruitment precedes monocyte recruitment to the dermal site of *L. major* infection (34), although by 48 h postinfection, monocytes made up a major proportion of skin-derived $CD11b^+$ cells (Fig. 3C and D, right). On day 9 p.i., $Ly6C^{hi}$ cells accounted for almost 50% of the $CD11b^+$ cells in the ear. In contrast, neutrophils and inflammatory monocytes made up a minor portion of $CD11b^+$ cells in the footpad at all time points tested following infection (Fig. 3C).

We wanted to directly compare the impacts of different routes of inoculation at the same anatomical site. However, the ear does not have a subcutaneous space, and i.d. injection into the footpad or other dermal sites, such as the flank, was not reliable (data not shown). Employing sand fly bites to induce intradermal tissue damage in the footpad or ear did reveal increases in the frequency of inflammatory cells at these sites that were similar to each other (Fig. 4) and to that observed in the ear following i.d. needle inoculation (compare Fig. 4 and 3C). Therefore, neutrophil recruitment appears to a be a hallmark of dermal sites of sand fly bite regardless of location, and i.d. needle inoculation of the ear most closely replicates this response.

Analysis of RFP^+ cells revealed that a greater proportion of $CD11b^+$ cells were infected in the ear than in the footpad at all time points tested (Fig. 5A, top) (P, ≤ 0.0018), and this correlated with an approximately 10-fold increase in the total number of

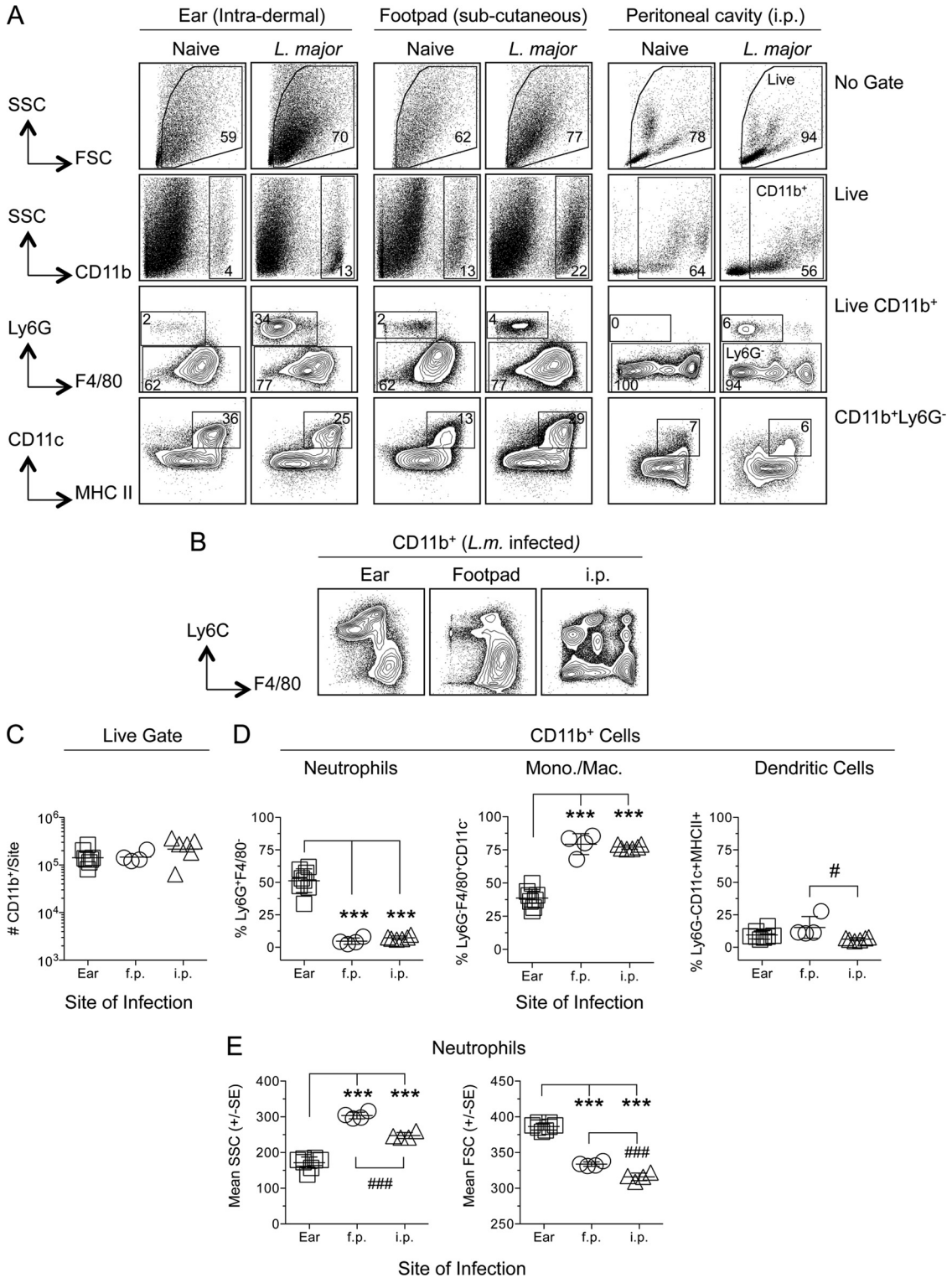

FIG 1 Phenotypic analysis of phagocytic cells following needle inoculation of the ear (intradermal), footpad (f.p.) (subcutaneous), or peritoneal cavity (i.p.) with *L. major*-RFP reveals site-specific populations of $CD11b^+$ cells. Individual C57BL/6 mice were injected with 1×10^6 *L. major*-RFP metacyclic promastigotes via the indicated route. Ten hours postinfection, cells from naïve or infected mice were prepared, stained for the indicated surface markers, and analyzed by flow cytometry. (A) Representative dot plots and gating strategy of phagocytic populations. (B) Equal portions of the individual samples for which results are reported in panels C and D were pooled, and the pooled samples were stained for the indicated surface markers and analyzed by flow cytometry. (C) Total relative number of $CD11b^+$ cells recovered from each site of analysis. Results for 8 (ear), 4 (f.p.), or 6 (i.p.) mice are shown. (D) Percentages of neutrophils ($CD11b^+$ $Ly6G^+$ $F4/80^-$), monocytes/macrophages ($CD11b^+$ $Ly6G^-$ [MHC-II $CD11c]^-$), or dendritic cells ($CD11b^+$ $Ly6G^-$ [MHC-II $CD11c]^+$) among total $CD11b^+$ cells. A log scale was employed here and elsewhere in order to display large differences in cell numbers accurately. (E) SSC and FSC characteristics of $CD11b^+$ $F4/80^-$ $Ly6G^+$ neutrophils derived from the ear, f.p., or peritoneal cavity 2 h following inoculation with 1×10^6 *L. major* parasites. Horizontal lines represent the means ± SD (C and D) or standard errors (E). Asterisks indicate a significant difference from the ear group; number signs indicate a significant difference from the f.p. group. The levels of significance represented by various numbers of asterisks are explained in Materials and Methods. Data are representative of 2 independent experiments.

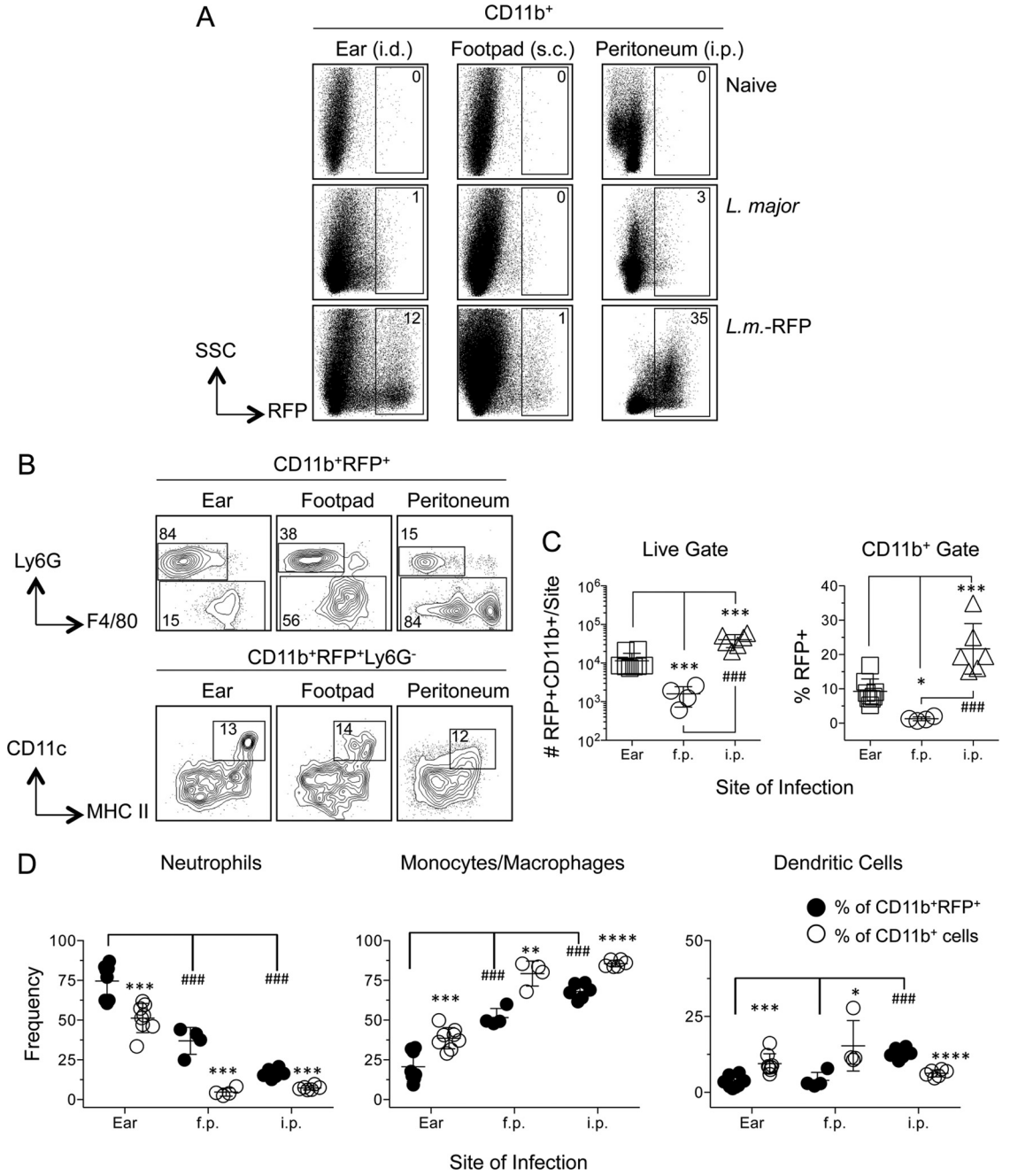

FIG 2 Phenotypic analysis of *L. major*-infected CD11b$^+$ RFP$^+$ cells in the ear (i.d.), footpad (s.c.), and peritoneal cavity reveals increased frequencies of infected neutrophils in the ear and preferential parasite capture by neutrophils. Samples for which results are shown in Fig. 1 were analyzed as a function of RFP expression. (A) Representative dot plots of RFP expression by CD11b$^+$ cells in naïve mice or in mice injected with wild-type or RFP-expressing *L. major* parasites. (B) Representative dot plots and gating strategy of CD11b$^+$ RFP$^+$ cells. (C) Total relative number of CD11b$^+$ RFP$^+$ cells (left) or frequency of RFP$^+$ cells within the CD11b$^+$ gate (right) as a function of site. (D) Frequencies of the indicated myeloid populations among total CD11b$^+$ RFP$^+$ cells (filled circles) or total CD11b$^+$ cells (open circles). Asterisks indicate a significant difference between total CD11b$^+$ cells and CD11b$^+$ RFP$^+$ cells. Number signs indicate a significant difference between groups as indicated by the brackets. Horizontal lines represent means ± SD. Data are representative of 2 independent experiments.

RFP$^+$ CD11b$^+$ cells (Fig. 5A, bottom) (P, ≤0.009). By day 9 p.i., the large increase in total CD11b$^+$ cells in the ear (Fig. 3A) (the data in Fig. 3 and 5 are from the same experiment) resulted in frequencies of infected CD11b$^+$ cells lower than those at the 48-h time point (Fig. 5A). At 2 and 48 h p.i., Ly6G$^+$ neutrophils represented a significantly larger proportion of RFP$^+$ CD11b$^+$ infected cells in the ear than in the footpad (P, <0.0001) (Fig. 5B, left and center, and C, center), where approximately 75% of infected cells were Ly6G$^-$ Ly6C$^{neg/lo}$ at all time points (Fig. 5B, bottom, and C, left). This was also reflected in the total number of infected cells (Fig. 5D). RFP$^+$ Ly6G$^-$ Ly6C$^{neg/lo}$ cells in the footpad contained low frequencies of CD11c$^+$ MHC-II$^+$ DCs at 2 and 48 h (Fig. 5E),

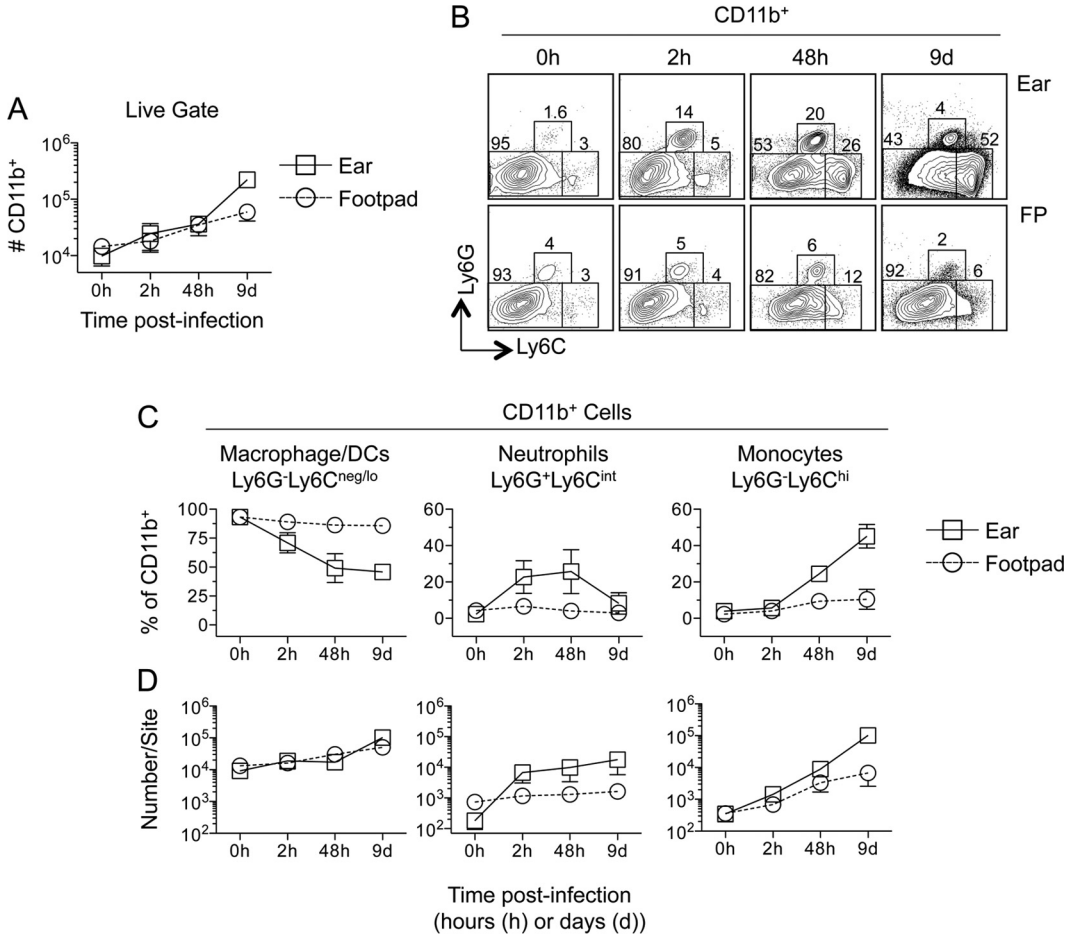

FIG 3 Kinetic analysis of myeloid cell recruitment reveals enhanced recruitment to the ear as opposed to the footpad following the inoculation of *L. major*-RFP. Mice were injected with 2.5×10^5 *L. major*-RFP parasites i.d. in the ear or s.c. in the footpad. At the indicated time points p.i., each site was analyzed for the indicated myeloid populations. (A) Total relative numbers of $CD11b^+$ cells at each site. d, day. (B) Representative dot plots of Ly6G and Ly6C expression on $CD11b^+$ cells. (C and D) Frequencies of the indicated myeloid populations among $CD11b^+$ cells (C) or total relative number of each population (D) at each site over the indicated time p.i. Data are means ± SD for 5 to 6 (ear) or 5 to 7 (f.p.) samples. Data are representative of 2 independent experiments.

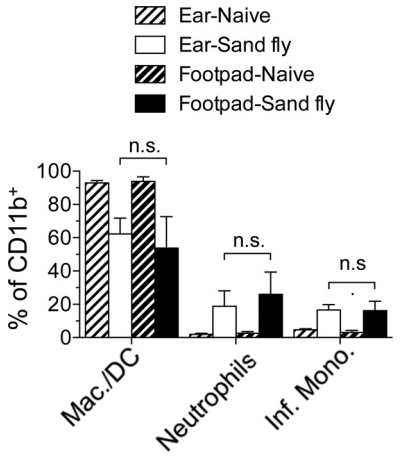

FIG 4 Sand fly bites elicit equivalent recruitment of inflammatory cells to the footpad or ear skin. Shown are the frequencies of $Ly6G^-$ $Ly6C^{neg/lo}$ macrophages/DCs, $CD11b^+$ $Ly6G^+$ $Ly6C^{intermediate}$ neutrophils, or $Ly6G^-$ $Ly6C^{hi}$ inflammatory (Inf.) monocytes among $CD11b^+$ cells 10 h following exposure to the bites of uninfected *P. duboscqi* sand flies. Data are means ± SD for 11 to 12 (sand fly-exposed ears or footpads) or 4 (naïve ears or footpads) samples. Data are pooled from 2 independent experiments with similar results. n.s., not significant.

suggesting that the majority of infected cells in the footpad at early time points are $CD11b^+$ $Ly6G^-$ $Ly6C^{neg/lo}$ $(CD11c\ MHC\text{-}II)^-$ macrophages.

Intradermal inoculation of the ear results in a higher effective dose than subcutaneous inoculation of the footpad. The findings presented above (Fig. 2C and 5A) suggest that there is a difference in the initial number of parasites that establishes infection between intradermal and subcutaneous sites. In order to confirm that the flow cytometric results reflected the relative number of viable organisms at each site, we repeated the experiment to include limiting dilution analysis (LDA) to determine the parasite load. The flow cytometric analysis again revealed significantly greater numbers of $CD11b^+$ RFP^+ cells in the ear than in the footpad at 10 h after infection with 1×10^6 or 2.5×10^5 *L. major* metacyclic promastigotes (Fig. 6A and B, left), a difference that became more substantial at 11 to 12 days p.i. At both the high- and lower-dose inocula, the skin yielded higher parasite loads than the footpad at both 10 h and 11 days (Fig. 6A and B, right). The difference between the higher numbers obtained by LDA and the numbers of $CD11b^+$ RFP^+ cells per site obtained by flow cytometry could be reduced by determining the absolute number of

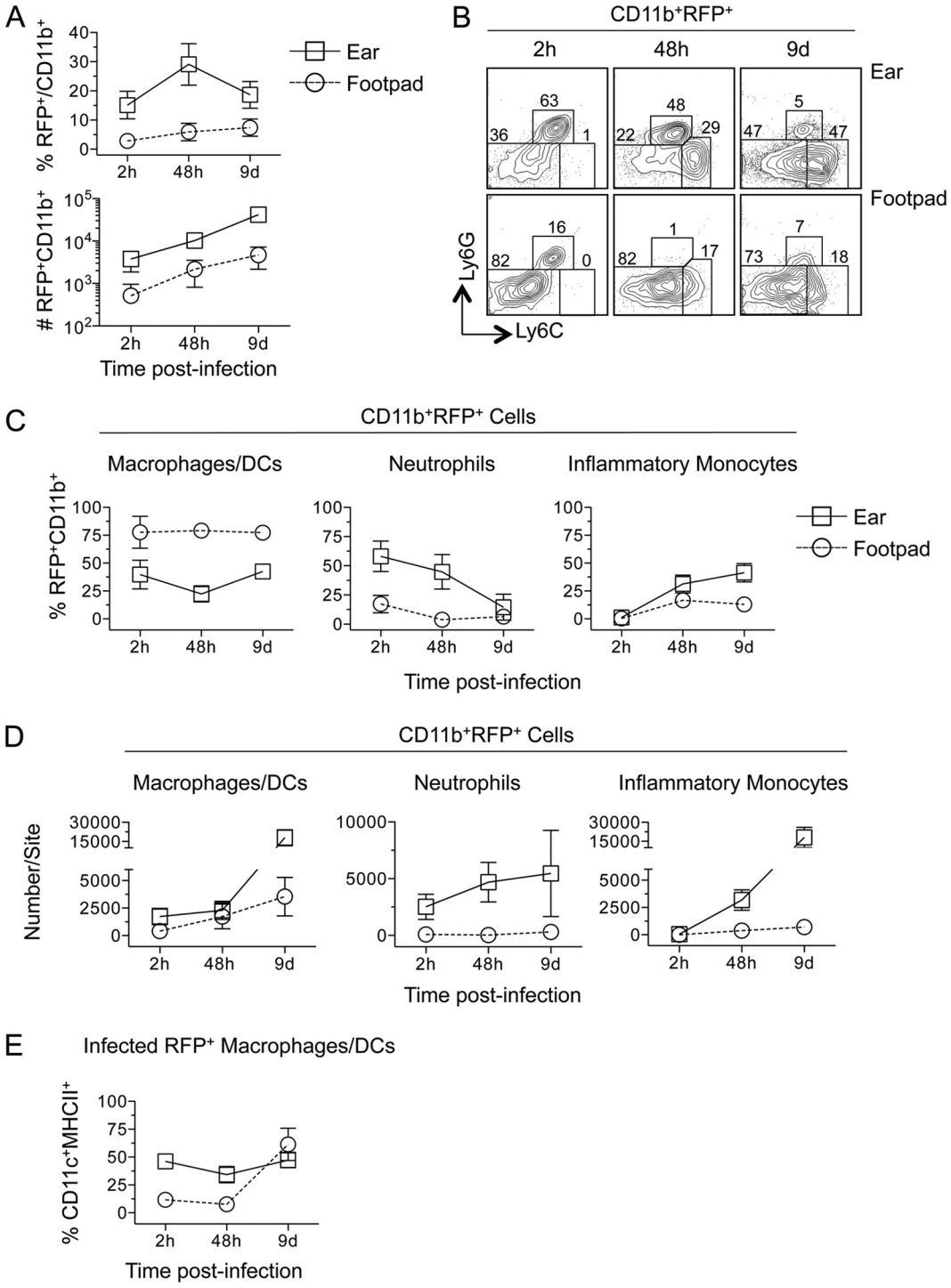

FIG 5 Increased neutrophil recruitment correlates with increased numbers of RFP^+ cells following i.d. inoculation of the ear versus s.c. inoculation of the footpad. Samples for which results are shown in Fig. 3 were analyzed as a function of RFP expression. (A) Frequency of infected (RFP^+) $CD11b^+$ cells among total $CD11b^+$ cells (top) or total relative number of $CD11b^+$ RFP^+ cells at each site over the indicated time p.i. (B) Representative dot plots of Ly6G and Ly6C expression on $CD11b^+$ RFP^+ cells. (C and D) Frequencies of the indicated myeloid populations among $CD11b^+$ RFP^+ cells (C) or total relative number of each population (D) at each site over the indicated time p.i. (E) Frequency of $CD11c^+$ MHC II^+ cells within the infected $CD11b^+$ $Ly6G^-$ $Ly6C^{lo}$ RFP^+ or $CD11b^+$ $Ly6G^-$ $Ly6C^{hi}$ RFP^+ population at each site over time. Each symbol represents the mean, and error bars represent SD, for 5 to 6 (ear) or 5 to 7 (f.p.) samples. Data are representative of 2 independent experiments.

$CD11b^+$ RFP^+ cells by use of counting beads, which increased the infected-cell counts approximately 4-fold on day 11 p.i. in both the ear and the footpad (Fig. 6C). Alternative gating strategies, including omission of the CD11b gate, did not significantly reduce the discrepancy between the number of RFP^+ cells and the LDA results (data not shown). In order to ensure that the difference in the number of parasites in the ear or footpad early following infection was not due to the relatively high doses required to follow

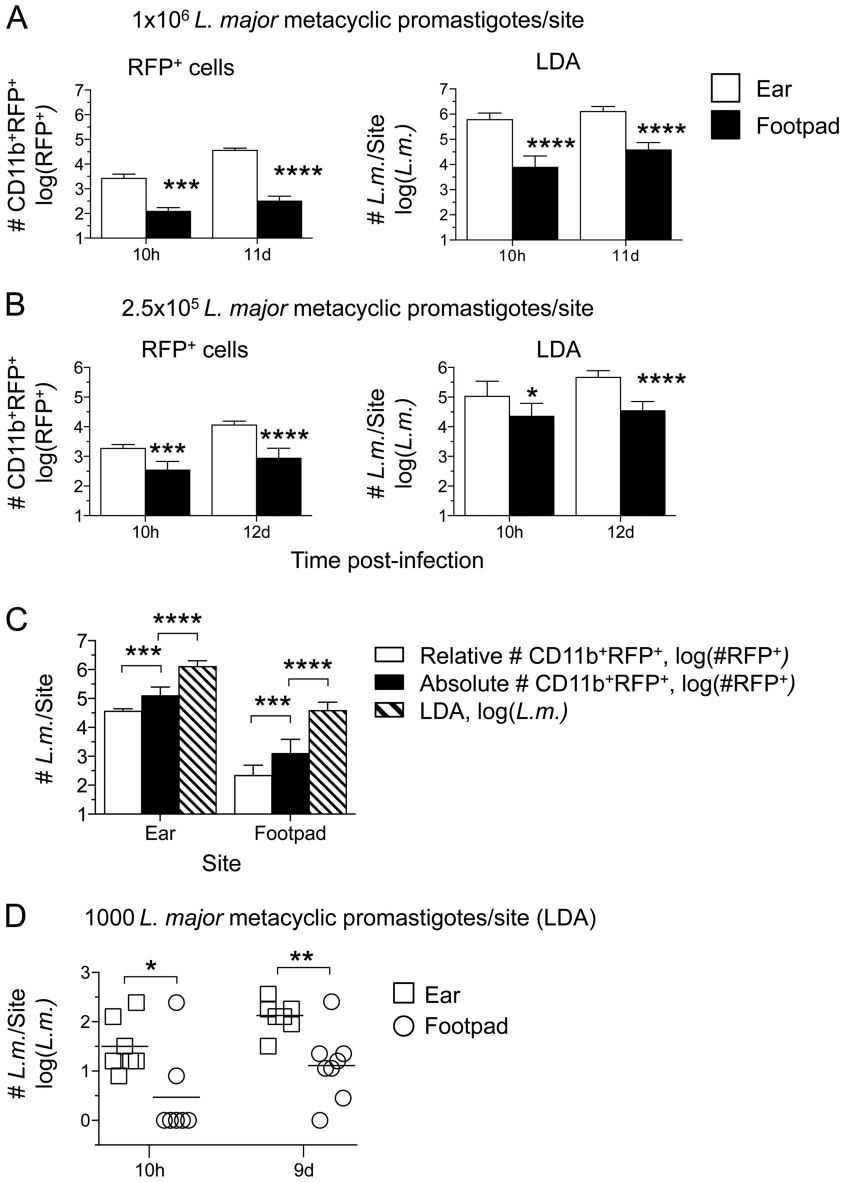

FIG 6 Intradermal inoculation of the ear results in a higher effective dose than s.c. inoculation of the footpad. Mice were infected i.d. in the ear or s.c. in the footpad with *L. major*-RFP. At the indicated time points, the number of $CD11b^+$ RFP^+ cells (RFP^+ cells), or the number of parasites as determined by limiting dilution analysis (LDA), per ear or footpad was determined. Analysis was performed following needle inoculation of 1×10^6 (A), 2.5×10^5 (B), or 1,000 (D) metacyclic promastigotes. (C) Day 12 p.i. data from the experiment for which results are shown in panel A were plotted with the absolute number of $CD11b^+$ RFP^+ cells per site as determined by employing counting beads. Six to 12 ears or footpads were analyzed per time point. Asterisks indicate a significant difference between the ear and footpad groups (A, B, and D) or between the groups indicated by brackets (C). (D) *, $P = 0.012$; **, $P = 0.008$.

RFP^+ cells by flow cytometry, we inoculated mice with 1,000 *L. major* metacyclic promastigotes s.c. or i.d., and the parasite load was determined by LDA only. Once again, i.d. inoculation of the ear resulted in significantly higher parasite loads, returning 13-fold- and 11-fold-greater numbers of parasites than the footpad at 10 h and 9 days, respectively (Fig. 6D).

Assessment of adaptive immunity following i.d. versus s.c. inoculation. We also wanted to determine if the dramatically larger parasite loads observed in the ear relative to the footpad influenced the onset or class of adaptive immunity at the site of infection. Analysis of IFN-γ mRNA levels following the inoculation of 2.5×10^5 parasites revealed higher levels in the ear than in the footpad, and these expression levels increased between 48 h and 9 days (Fig. 7A). Flow cytometric analysis also revealed a higher frequency and number of $CD4^+$ IFN-γ^+ cells in the ear than in the footpad on day 12 p.i. (Fig. 7B). These results strongly suggest that the lower parasite loads observed in the footpad at day 10 p.i. are not due to an enhanced adaptive immune response. We also found low levels of interleukin 4 (IL-4), IL-17, and IL-10 gene expression in both the ear and the footpad, suggesting that the lack of IFN-γ production in the footpad is due to the lower parasite loads at this site and not to immune deviation. Following inoculation of a low dose (1,000 parasites), we did not detect any IFN-γ^+ T cells in the footpad or the ear on day 9 p.i. (Fig. 7C) and

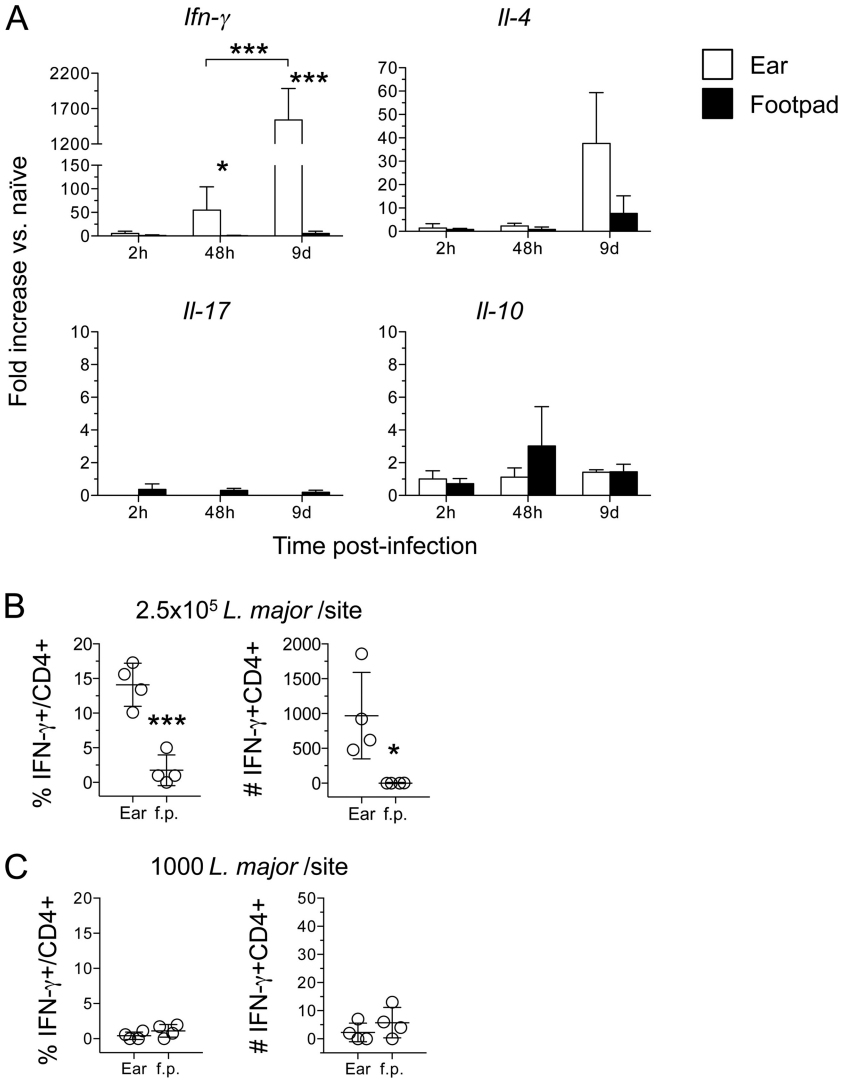

FIG 7 Decreased parasite numbers following s.c. inoculation of the footpad are not due to earlier onset of adaptive immunity. (A) Total RNA was isolated directly from the ears or footpads for which results are shown in Fig. 3, reverse transcribed, and analyzed by real-time PCR. The expression of the target genes was normalized to that of an endogenous control, and the values shown are fold increases over expression in naïve ears or footpads. Data are means ± SD for 3 to 5 samples. (B and C) Intracellular staining for IFN-γ. The $CD3^+$ $CD4^+$ T cells used were from ear or footpad samples for which results are shown in Fig. 6B, day 12 (B), or in Fig. 6D, day 9 (C). Asterisks indicate a significant difference between the ear and footpad groups or between the groups indicated by brackets. Data are means ± SD for 4 samples.

did not detect IFN-γ by enzyme-linked immunosorbent assay (ELISA) following 72-h antigen restimulation (data not shown). This was despite the 11-fold-higher parasite numbers in the ear than in the footpad (Fig. 6D). The increased level of IL-4 gene expression at day 9 p.i. in the ear (Fig. 7A) was not a consistent finding.

A significant portion of needle-inoculated parasites fail to establish infection in the absence of neutrophils. Our observations suggest that large numbers of inoculated parasites are dependent on the recruitment of neutrophils in order to establish infection, similar to our previous observations following transmission by sand fly bite (33). We wanted to demonstrate this formally by depleting neutrophils prior to inoculation. However, our extensive observations employing the neutrophil-depleting antibodies 1A8, RB6-8C5, and NIMP-R14 revealed that none of these reagents performed in an ideal manner (Fig. 8A to C). RB6-8C5 was highly efficient at depleting $Ly6G^+$ $Ly6C^{intermediate}$ neutrophils but also depleted $Ly6G^-$ $Ly6C^{hi}$ inflammatory monocytes (Fig. 8A). Similar results were obtained with NIMP-R14. Treatment with 1A8 was more specific to neutrophils, with no observed depletion of $Ly6C^{hi}$ $GR1^{intermediate}$ monocytes. However, while administration of 1A8 did significantly reduce neutrophil numbers and frequencies in the ear, it was also found to be inefficient, with significant numbers of dermal neutrophils remaining (Fig. 8B). The inefficiency of neutrophil depletion by 1A8 was most apparent in the blood, where the frequency of neutrophils was reduced by only 2.3-fold (Fig. 8C). In some experiments, treatment with 1A8 reduced the number of neutrophils in the ear following *L. major* challenge by only 50% (data not shown). Keeping these caveats in mind, we determined the number of parasites that was able to establish infection 16 h after challenge of mice pretreated with Ab 1A8 or RB6-8C5. In both cases, Ab treatment reduced the total

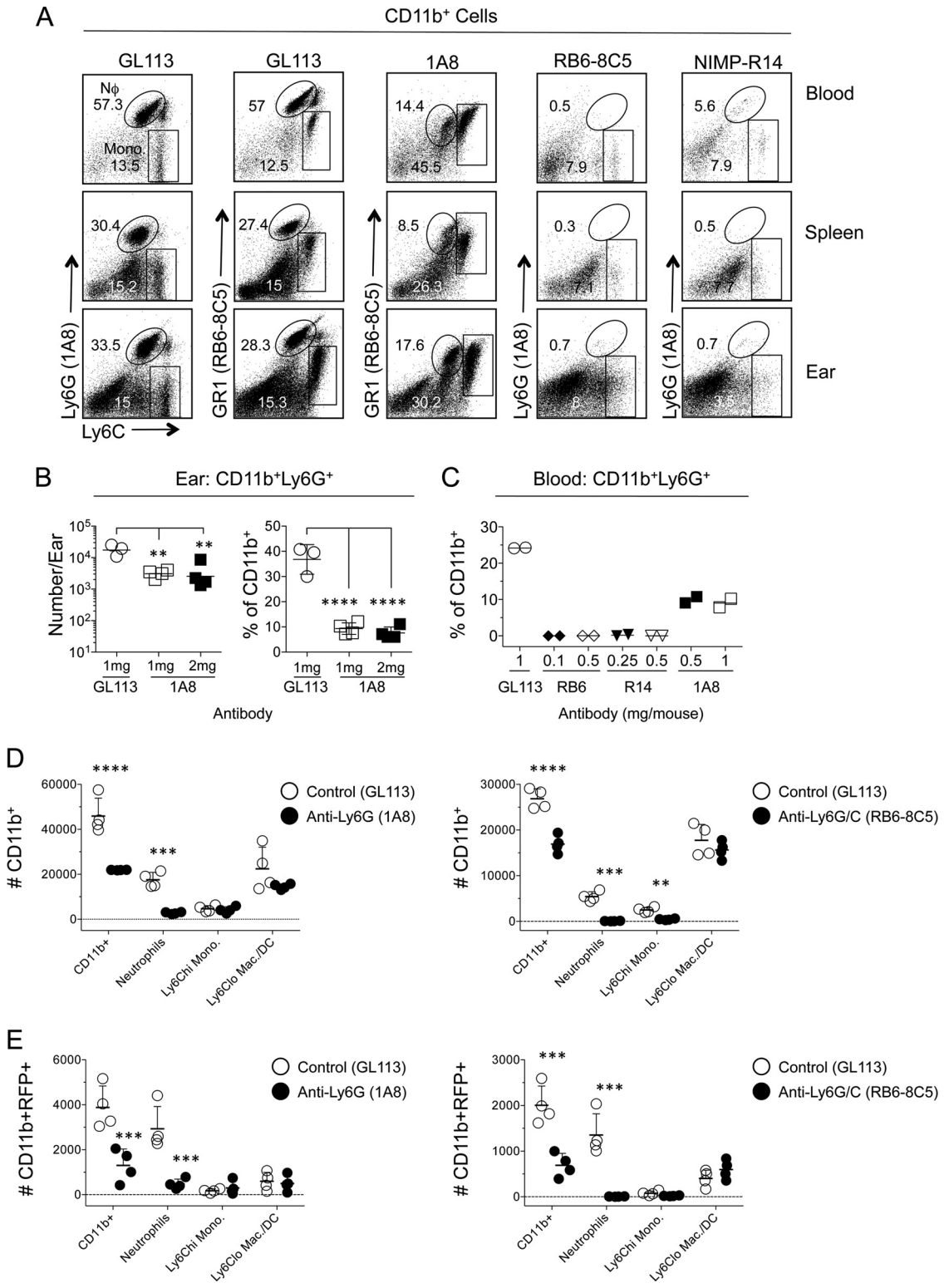

FIG 8 A significant portion of needle-inoculated parasites fail to establish infection in the absence of neutrophils. (A to E) Mice were injected i.p. with antibody 1A8, RB6-8C5, or NIMP-R14 prior to needle inoculation of the ear with 7.5×10^5 to 1×10^6 *L. major* metacyclic-promastigotes. Sixteen hours p.i., $CD11b^+$ cells from the ear, spleen, and blood were assessed for CD11b, Ly6G, and Ly6C expression. (A) Representative dot plots of Ly6C and Ly6G expression on $CD11b^+$ cells from mice treated with 0.5 mg of antibody 24 h prior to *L. major* inoculation. (B) Total relative number (left) or frequency (right) of $CD11b^+$ $Ly6G^+$ cells in the ears of mice treated with Ab 1A8. Mice received either a single 1-mg dose of 1A8 24 h prior to challenge or two 1-mg doses of 1A8, one at 24 h and one at 48 h prior to challenge. Horizontal lines indicate means ± SD for 3 to 4 mice per experiment. (C) Percentages of $CD11b^+$ $Ly6G^+$ neutrophils in the blood of mice treated with the indicated doses of antibodies 24 h prior to challenge. (D and E) Mice were treated with the antibody 1A8 (left) or RB6-8C5 (right) 24 h prior to injection with *L. major*. Ears were analyzed for the total relative numbers of the indicated $CD11b^+$ (D) or $CD11b^+$ RFP^+ (E) myeloid populations. Horizontal lines represent means ± SD for 4 mice. Data are representative of 2 independent experiments. Asterisks indicate a significant difference between groups as indicated by the brackets (B) or between GL113 and IA8- or RB6-8C5-treated mice for each cellular phenotype (D and E). Similar data were obtained by employing 0.5 or 1 mg of antibody.

number of $CD11b^+$ cells and the number of $CD11b^+$ $Ly6G^+$ neutrophils per ear (Fig. 8D) and reduced the number of infected $CD11b^+$ cells approximately 3-fold (Fig. 8E). It should be noted that 1A8 depletion of neutrophils in this experiment represents a best-case scenario. Although RB6-8C5 significantly reduced the total number of $Ly6C^{hi}$ monocytes in the ear, this did not lead to a significant reduction in the number of RFP^+ $Ly6C^{hi}$ monocytes, since monocytes represent a small fraction of infected cells at this time point. In addition, infection established in the absence of neutrophils did not significantly increase the number of infected $Ly6C^{hi}$ monocytes or $Ly6C^{neg/lo}$ macrophages/DCs, suggesting that a large number of parasites are dependent on neutrophil recruitment to establish infection, a pattern similar to what we have demonstrated following an infected sand fly bite (33).

Macrophages are the primary infected cell type in the peritoneal cavity during acute infection. While the peritoneal cavity is not a physiological site of *L. major* infection, previous work (35) employed infection at this site to demonstrate that inflammatory monocytes phagocytose a significant number of parasites and, in contrast to what has been reported for neutrophils (33), are able to kill *L. major*. However, we found that the peritoneal cavity returned the highest number and frequency of infected cells at 10 h p.i. Therefore, we investigated the proportion of $CD11b^+$ RFP^+ cells that are inflammatory monocytes at the acute time points employed by Goncalves et al. (35). As shown previously (35), and in contrast to the findings for the ear (34), the recruitment of $Ly6C^{hi}$ inflammatory monocytes preceded that of $Ly6G^+$ neutrophils at 1 h p.i. (Fig. 9A and B) (P, <0.0001). However, while the number of monocytes increased 4.6-fold between 1 and 4 h p.i. (P, 0.016), there was an even larger, 218-fold increase in the number of neutrophils during this time (P, 0.0084). Neither recruited population outnumbered the largely preexisting $CD11b^+$ $Ly6G^-$ $Ly6C^-$ resident macrophage/DC populations (Fig. 9B). Analysis of $CD11b^+$ RFP^+ cells revealed that $Ly6C^{hi}$ inflammatory monocytes represented less than 1% of infected cells at both 1 and 4 h p.i., while the proportion of infected neutrophils increased slightly, from 1% to 8% (Fig. 9C and D). In contrast, at 1 h p.i., the vast majority of RFP^+ $CD11b^+$ cells were preexisting $Ly6G^-$ $Ly6C^-$ $F4/80^{high}$ cells, followed by $Ly6G^-$ $Ly6C^-$ $F4/80^{intermediate}$ $MHC\text{-}II^{high}$ cells, and this proportion did not change significantly at 4 h p.i. (Fig. 9D), a pattern similar to what we observed at 10 h p.i. (Fig. 2D). Therefore, the high levels of infection in the peritoneal cavity appear to be the result of efficient phagocytosis of *L. major* by largely preexisting $F4/80^{high}$ peritoneal macrophages, and in striking contrast to i.d. inoculation of the ear, recruited neutrophils or inflammatory monocytes appear to play a small role in initial parasite uptake at this site. We have shown previously that diminished RFP expression correlates with increased parasite death, as evidenced by uptake of a dead cell dye and expression of phospholipids (33). In contrast to previous studies in which the number of RFP-expressing $Ly6C^{hi}$ monocytes dropped significantly between 1 and 4 h (35), we found no evidence of parasite killing by infected inflammatory monocytes in the peritoneal cavity (Fig. 9E).

DISCUSSION

Intradermal needle inoculation of the ear has been extensively employed as the route of infection that most closely replicates the physiological intradermal and intraepidermal deposition of parasites by the bite of an infected sand fly. However, whether this effort to reproduce the natural site of inoculation has significant consequences for infection outcome had not been studied in detail. Following deposition into the skin by an infected sand fly bite, *L. major* parasites are tightly associated with neutrophils, and 3-dimensional (3-D) imaging has revealed that the majority of parasites are phagocytosed by neutrophils (33, 38). Employing an RFP-expressing *L. major* parasite and multicolor flow cytometric analysis, we found that phenotypic differences in preexisting and recruited populations of phagocytic cells at different sites of inoculation significantly influence the establishment of infection. Similar to physiological transmission by sand fly bite, i.d. inoculation of the ear, but not i.p. inoculation or s.c. inoculation of the footpad, resulted in a high frequency of recruited neutrophils. Neutrophils were the predominant infected cells at acute time points p.i. in the ear and, regardless of site, were overrepresented as a proportion of infected cells relative to their proportion of total $CD11b^+$ cells. Furthermore, upon treatment of mice with neutrophil-depleting antibodies, significantly fewer parasites were able to establish infection. The differences in infected cell numbers and infected cell phenotypes observed following i.d. versus s.c. inoculation were not due to altered kinetics. In addition, the larger number of parasites that established infection in the ear as a result of neutrophil recruitment was maintained for at least 12 days p.i. and appeared to become more significant with time. Therefore, the effort to replicate sand fly-mediated transmission using the i.d. route of needle inoculation has significant consequences for the establishment of infection.

The route of pathogen, vaccine, or protein delivery has often been cited as an important factor in the outcome of infection or the induction of immunity (1–19, 20–31, 40–42). For example, injection of hen egg lysozyme (HEL) protein i.p. or s.c. leads to the generation of $CD4^+$ T cells with different cytokine profiles and different peptide specificities (42). These differences have been attributed to differences in the abilities of diverse antigen-presenting cells at different sites to process and present peptides from the HEL protein (43). It has been suggested that enhanced T cell priming by skin-resident DCs and Langerhans cells is the reason why intradermal vaccine inoculation is often superior to intramuscular inoculation (18, 19). The influence of the inoculation site on the outcome of *L. major* infection has been studied largely in the context of site-dependent adaptive immunity, irrespective of dose, and typically with reference to the Th1/Th2 nature of responding $CD4^+$ T cells or the production of the regulatory cytokine IL-10 or transforming growth factor β (TGF-β) (1, 3–5, 7–9, 41). Here we demonstrate that even before different antigen-presenting cells begin to prime adaptive immunity, the site of inoculation immediately influences the effective dose of *L. major* parasites that establishes infection. The parasite dose has far-reaching implications for *Leishmania* infections, including the nature of the adaptive immune response, and is likely one of the most important variables in determining the kinetics and outcome of infection (6, 36, 44–48). Our observations demonstrate that the number of parasites that establishes infection must be considered in interpreting the influence of the site of infection, as suggested previously (6). We and others have demonstrated that the relative differences in parasite load or lesion size following inoculation at different sites or with different doses of parasites can change depending on the time of analysis (1, 3, 7, 36, 48). For example, while we observed earlier control of parasite numbers in the ear than in the footpad, likely due to the earlier onset of adaptive immunity as

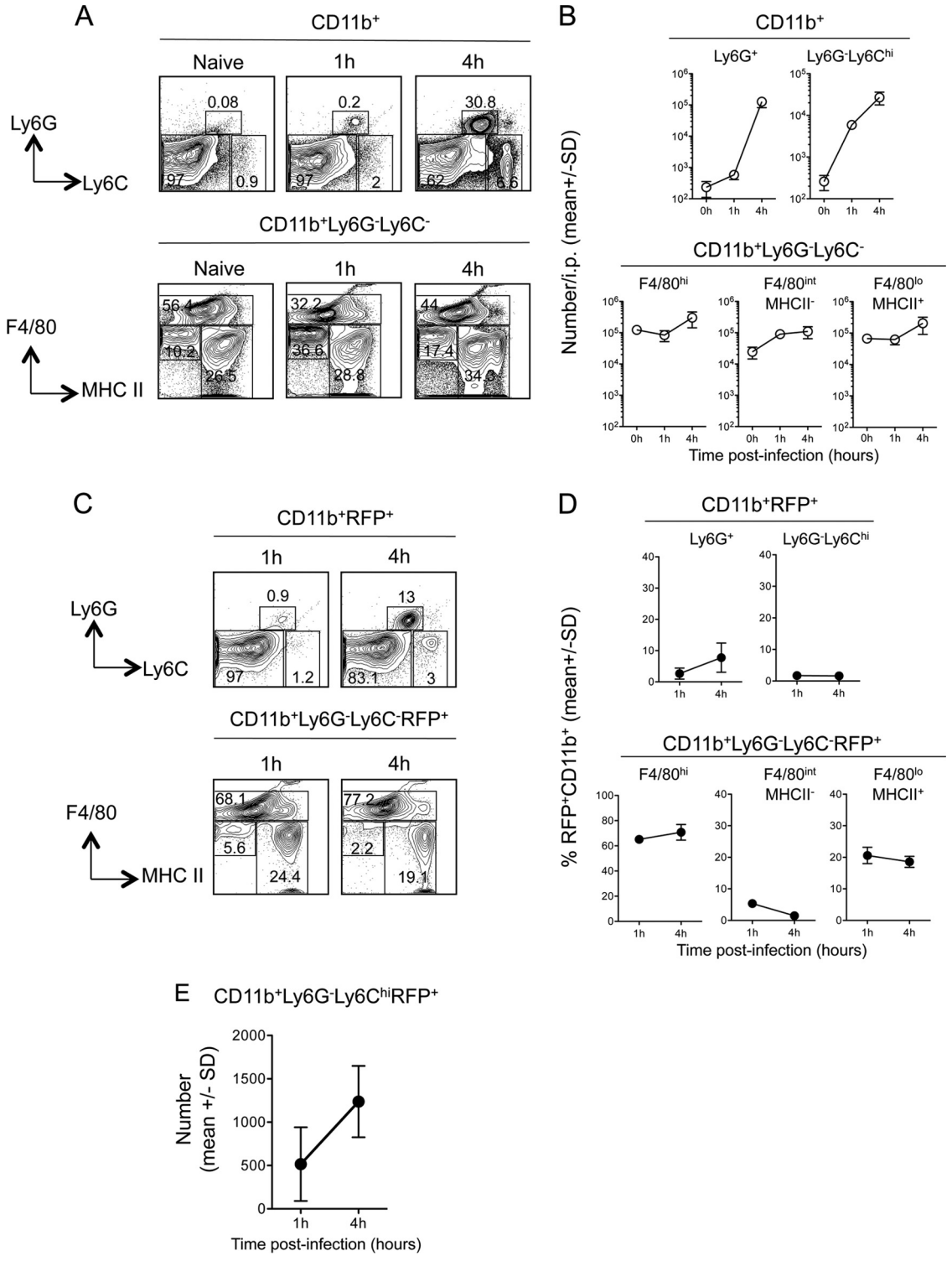

FIG 9 Analysis of total and infected CD11b$^+$ myeloid populations in the peritoneal cavity reveals that inflammatory monocytes are rapidly recruited but phagocytose relatively few parasites. Mice were injected i.p. with 2×10^6 *L. major*-RFP parasites, and at the indicated time points p.i., myeloid cells were analyzed for RFP expression. (A) Representative dot plots and gating strategy of CD11b$^+$ cells. (B) Total relative numbers of the indicated myeloid populations per cavity. Results for 3 mice are shown. (C) Representative dot plots and gating strategy of CD11b$^+$ RFP$^+$ cells. (D) Frequencies of the indicated myeloid populations among total CD11b$^+$ RFP$^+$ cells. (E) Total relative numbers of infected (RFP$^+$) inflammatory monocytes in the peritoneal cavity at 1 and 4 h p.i. Symbols represent means; error bars indicate SD. Data are representative of 2 independent experiments.

shown here, a 10-fold-higher parasite load was maintained in the ear during chronic infection (3). Other factors, such as host cell permissiveness and regulatory cytokine production, may also be involved in the outcomes of infection at different sites. Interestingly, our results suggest that a direct comparison of non-dose-related effects of i.d. ear versus s.c. footpad inoculation would require the injection of approximately 10-fold greater numbers of parasites into the footpad.

While neutrophils downmodulate infected DCs at i.d. sites of *L. major* inoculation, resulting in a decreased capacity to prime $CD4^+$ T cells (34), the massive increase in the number of parasites that established infection in the presence of neutrophils following i.d. inoculation of the ear over that following s.c. inoculation of the footpad with large doses of parasites resulted in the earlier onset of adaptive immunity. Initiation of adaptive immunity following i.d. infection of the ear dermis by the same number of parasites in the absence of neutrophils would likely result in even greater enhancement of the adaptive response.

Because we are unable to reliably confine our footpad injections to the dermis, we employed sand fly bites to elicit physiologically relevant tissue damage of the ear or footpad dermis and found the frequencies of neutrophils to be similar. Therefore, the preponderance of neutrophils associated with sand fly bites or i.d. needle inoculation of the ear appears to be a general characteristic of i.d. tissue damage. By comparing the i.d. route of infection in the ear and the neutrophil-deficient s.c. route of infection in the footpad, we were able to show a role for neutrophils in determining the number of parasites that establishes infection at the tissue site. This was reinforced by experiments carried out in the ear dermis employing neutrophil-depleting antibodies, which, despite the caveats associated with either incomplete or nonspecific depletion, showed clear reductions in the numbers of infected cells at early time points. In addition to their preferential recruitment, the overrepresentation of neutrophils among infected versus total $CD11b^+$ cells in the dermis also suggests that their mobility or phagocytic capacity gives them a distinct advantage over other phagocytic cell types in capturing *L. major* parasites.

We found that limiting dilution analysis (LDA) returned higher total parasite loads than detection of RFP^+ cells. This difference could be attributed partly to cell loss during the preparation of cells for flow cytometric analysis, as indicated by the 4-fold increase in the number of RFP^+ cells following numerical adjustment employing counting beads. Other factors, such as specific loss of heavily infected or infected apoptotic cells during the staining procedure, exclusion of RFP^+ doublets during postacquisition analysis, exclusion of dying infected neutrophils, loss of parasites that are transitioning from infected neutrophils to other phagocytic cells via a cell release mechanism (33), and the fact that LDA is performed after a single high-speed centrifuge spin, resulting in minimal loss of viable parasites, all likely contribute to this discrepancy. While LDA returned higher parasite loads, the relationships between the different groups remained the same regardless of the methodology employed to determine parasite loads.

Inoculation of the peritoneal cavity resulted in the highest initial parasite loads, but in contrast to neutrophil-dependent uptake in the ear dermis, this was due in large part to phagocytosis by $F4/80^{high}$ peritoneal macrophages, an infected population unique to this site and, at 1 h postinfection, an entirely preexisting population. The uptake of *L. major* by preexisting cells is similar to what has been reported for the lung, another nonphysiological site of infection (41). Our observations would suggest that the peritoneal cavity, or cells derived from the peritoneal cavity, should be used with caution in the context of *Leishmania* studies, since the phenotype, recruitment, and morphology of cells derived from this site are considerably different from those observed following i.d. infection. This is especially true of infected peritoneal macrophages, which do not appear to have a phenotypic counterpart in the skin yet phagocytose the majority of parasites following i.p. inoculation.

The skin is a critical barrier organ that possesses redundant mechanisms to initiate a wound-healing response. Vector-borne infections that are initiated in the skin are likely to involve adaptations to this unique microenvironment by the invading pathogen (29). Bypassing or altering this initial step in infection is likely to have significant and unforeseen consequences, such as those observed here. In this regard, inoculation of the footpad is sometimes referred to as a cutaneous or dermal route of infection; however, the subcutaneous space is physiologically and functionally distinct from the dermis and epidermis. In the case of leishmaniasis, the use of the intradermal model of needle inoculation has provided critical evidence to support observations employing natural transmission of the parasite by infected sand flies. This evidence has provided insight into the unique adaptations that *Leishmania* has undergone to survive and even exploit the potent neutrophil host response to a breach of the skin barrier following a sand fly bite.

ACKNOWLEDGMENTS

This research was supported by the Intramural Research Program of the NIH, National Institute of Allergy and Infectious Diseases. Financial support was provided by the NIH-CAPES sandwich program to Eric Henrique Roma (CAPES no. 0062/11-1) and Matheus B. H. Carneiro (CAPES no. 8619/12-3).

We thank Kimberly Beacht for assistance with experiments.

REFERENCES

1. **Mahmoudzadeh-Niknam H, Khalili G, Abrishami F, Najafy A, Khaze V.** 2013. The route of *Leishmania tropica* infection determines disease outcome and protection against *Leishmania major* in BALB/c mice. Korean J. Parasitol. **51:**69–74. http://dx.doi.org/10.3347/kjp.2013.51.1.69.
2. **Oliveira DM, Costa MA, Chavez-Fumagalli MA, Valadares DG, Duarte MC, Costa LE, Martins VT, Gomes RF, Melo MN, Soto M, Tavares CA, Coelho EA.** 2012. Evaluation of parasitological and immunological parameters of *Leishmania chagasi* infection in BALB/c mice using different doses and routes of inoculation of parasites. Parasitol. Res. **110:**1277–1285. http://dx.doi.org/10.1007/s00436-011-2628-5.
3. **Tabbara KS, Peters NC, Afrin F, Mendez S, Bertholet S, Belkaid Y, Sacks DL.** 2005. Conditions influencing the efficacy of vaccination with live organisms against *Leishmania major* infection. Infect. Immun. **73:** 4714–4722. http://dx.doi.org/10.1128/IAI.73.8.4714-4722.2005.
4. **Osorio Y, Melby PC, Pirmez C, Chandrasekar B, Guarin N, Travi BL.** 2003. The site of cutaneous infection influences the immunological response and clinical outcome of hamsters infected with *Leishmania panamensis*. Parasite Immunol. **25:**139–148. http://dx.doi.org/10.1046/j.1365-3024.2003.00615.x.
5. **Baldwin TM, Elso C, Curtis J, Buckingham L, Handman E.** 2003. The site of *Leishmania major* infection determines disease severity and immune responses. Infect. Immun. **71:**6830–6834. http://dx.doi.org/10.1128/IAI.71.12.6830-6834.2003.
6. **Menon JN, Bretscher PA.** 1998. Parasite dose determines the Th1/Th2 nature of the response to *Leishmania major* independently of infection route and strain of host or parasite. Eur. J. Immunol. **28:**4020–4028. http://dx.doi.org/10.1002/(SICI)1521-4141(199812)28:12<4020::AID-IMMU4020>3.0.CO;2-3.
7. **Nabors GS, Farrell JP.** 1994. Site-specific immunity to *Leishmania major*

in SWR mice: the site of infection influences susceptibility and expression of the antileishmanial immune response. Infect. Immun. **62:**3655–3662.
8. **Nabors GS, Nolan T, Croop W, Li J, Farrell JP.** 1995. The influence of the site of parasite inoculation on the development of Th1 and Th2 type immune responses in (BALB/c × C57BL/6) F_1 mice infected with *Leishmania major*. Parasite Immunol. **17:**569–579. http://dx.doi.org/10.1111/j.1365-3024.1995.tb01000.x.
9. **Kirkpatrick CE, Nolan TJ, Farrell JP.** 1987. Rate of *Leishmania*-induced skin-lesion development in rodents depends on the site of inoculation. Parasitology **94**(Part 3)**:**451–465. http://dx.doi.org/10.1017/S0031182000055803.
10. **Johnson AM.** 1984. Strain-dependent, route of challenge-dependent, murine susceptibility to toxoplasmosis. Z. Parasitenkd. **70:**303–309. http://dx.doi.org/10.1007/BF00927816.
11. **Vaughan JA, Scheller LF, Wirtz RA, Azad AF.** 1999. Infectivity of *Plasmodium berghei* sporozoites delivered by intravenous inoculation versus mosquito bite: implications for sporozoite vaccine trials. Infect. Immun. **67:**4285–4289.
12. **Kernbauer E, Maier V, Rauch I, Muller M, Decker T.** 2013. Route of infection determines the impact of type I interferons on innate immunity to *Listeria monocytogenes*. PLoS One **8:**e65007. http://dx.doi.org/10.1371/journal.pone.0065007.
13. **Wollert T, Pasche B, Rochon M, Deppenmeier S, van den Heuvel J, Gruber AD, Heinz DW, Lengeling A, Schubert WD.** 2007. Extending the host range of *Listeria monocytogenes* by rational protein design. Cell **129:**891–902. http://dx.doi.org/10.1016/j.cell.2007.03.049.
14. **Pepper M, Linehan JL, Pagán AJ, Zell T, Dileepan T, Cleary PP, Jenkins MK.** 2010. Different routes of bacterial infection induce long-lived TH1 memory cells and short-lived TH17 cells. Nat. Immunol. **11:**83–89. http://dx.doi.org/10.1038/ni.1826.
15. **de Souza MS, Smith AL, Beck DS, Kim LJ, Hansen GM, Jr, Barthold SW.** 1993. Variant responses of mice to *Borrelia burgdorferi* depending on the site of intradermal inoculation. Infect. Immun. **61:**4493–4497.
16. **Yetter RA, Lehrer S, Ramphal R, Small PA, Jr.** 1980. Outcome of influenza infection: effect of site of initial infection and heterotypic immunity. Infect. Immun. **29:**654–662.
17. **Bodewes R, Kreijtz JH, van Amerongen G, Hillaire ML, Vogelzang-van Trierum SE, Nieuwkoop NJ, van Run P, Kuiken T, Fouchier RA, Osterhaus AD, Rimmelzwaan GF.** 2013. Infection of the upper respiratory tract with seasonal influenza A(H3N2) virus induces protective immunity in ferrets against infection with A(H1N1)pdm09 virus after intranasal, but not intratracheal, inoculation. J. Virol. **87:**4293–4301. http://dx.doi.org/10.1128/JVI.02536-12.
18. **Bhowmick S, Mazumdar T, Ali N.** 2009. Vaccination route that induces transforming growth factor beta production fails to elicit protective immunity against *Leishmania donovani* infection. Infect. Immun. **77:**1514–1523. http://dx.doi.org/10.1128/IAI.01739-07.
19. **Méndez S, Belkaid Y, Seder RA, Sacks D.** 2002. Optimization of DNA vaccination against cutaneous leishmaniasis. Vaccine **20:**3702–3708. http://dx.doi.org/10.1016/S0264-410X(02)00376-6.
20. **Qiu J, Yan L, Chen J, Chen CY, Shen L, Letvin NL, Haynes BF, Freitag N, Rong L, Frencher JT, Huang D, Wang X, Chen ZW.** 2011. Intranasal vaccination with the recombinant *Listeria monocytogenes* Δ*actA prfA** mutant elicits robust systemic and pulmonary cellular responses and secretory mucosal IgA. Clin. Vaccine Immunol. **18:**640–646. http://dx.doi.org/10.1128/CVI.00254-10.
21. **Mullins DW, Sheasley SL, Ream RM, Bullock TN, Fu YX, Engelhard VH.** 2003. Route of immunization with peptide-pulsed dendritic cells controls the distribution of memory and effector T cells in lymphoid tissues and determines the pattern of regional tumor control. J. Exp. Med. **198:**1023–1034. http://dx.doi.org/10.1084/jem.20021348.
22. **Lefford MJ.** 1977. Induction and expression of immunity after BCG immunization. Infect. Immun. **18:**646–653.
23. **Lefford MJ, Warner S, Amell L.** 1979. *Listeria* pneumonitis: influence of route of immunization on resistance to airborne infection. Infect. Immun. **25:**672–679.
24. **Thatte J, Rath S, Bal V.** 1995. Analysis of immunization route-related variation in the immune response to heat-killed *Salmonella typhimurium* in mice. Infect. Immun. **63:**99–103.
25. **Mohanan D, Slutter B, Henriksen-Lacey M, Jiskoot W, Bouwstra JA, Perrie Y, Kundig TM, Gander B, Johansen P.** 2010. Administration routes affect the quality of immune responses: a cross-sectional evaluation of particulate antigen-delivery systems. J. Controlled Release **147:**342–349. http://dx.doi.org/10.1016/j.jconrel.2010.08.012.
26. **Hurpin C, Rotarioa C, Bisceglia H, Chevalier M, Tartaglia J, Erdile L.** 1998. The mode of presentation and route of administration are critical for the induction of immune responses to p53 and antitumor immunity. Vaccine **16:**208–215. http://dx.doi.org/10.1016/S0264-410X(97)00190-4.
27. **Ohlfest JR, Andersen BM, Litterman AJ, Xia J, Pennell CA, Swier LE, Salazar AM, Olin MR.** 2013. Vaccine injection site matters: qualitative and quantitative defects in CD8 T cells primed as a function of proximity to the tumor in a murine glioma model. J. Immunol. **190:**613–620. http://dx.doi.org/10.4049/jimmunol.1201557.
28. **Budimir N, de Haan A, Meijerhof T, Gostick E, Price DA, Huckriede A, Wilschut J.** 2013. Heterosubtypic cross-protection induced by whole inactivated influenza virus vaccine in mice: influence of the route of vaccine administration. Influenza Other Respir. Viruses **7:**1202–1209. http://dx.doi.org/10.1111/irv.12142.
29. **Frischknecht F.** 2007. The skin as interface in the transmission of arthropod-borne pathogens. Cell. Microbiol. **9:**1630–1640. http://dx.doi.org/10.1111/j.1462-5822.2007.00955.x.
30. **Guilbride DL, Guilbride PD, Gawlinski P.** 2012. Malaria's deadly secret: a skin stage. Trends Parasitol. **28:**142–150. http://dx.doi.org/10.1016/j.pt.2012.01.002.
31. **Bosio CF, Jarrett CO, Gardner D, Hinnebusch BJ.** 2012. Kinetics of innate immune response to *Yersinia pestis* after intradermal infection in a mouse model. Infect. Immun. **80:**4034–4045. http://dx.doi.org/10.1128/IAI.00606-12.
32. **Peters NC, Sacks DL.** 2009. The impact of vector-mediated neutrophil recruitment on cutaneous leishmaniasis. Cell. Microbiol. **11:**1290–1296. http://dx.doi.org/10.1111/j.1462-5822.2009.01348.x.
33. **Peters NC, Egen JG, Secundino N, Debrabant A, Kimblin N, Kamhawi S, Lawyer P, Fay MP, Germain RN, Sacks D.** 2008. In vivo imaging reveals an essential role for neutrophils in leishmaniasis transmitted by sand flies. Science **321:**970–974. http://dx.doi.org/10.1126/science.1159194.
34. **Ribeiro-Gomes FL, Peters NC, Debrabant A, Sacks DL.** 2012. Efficient capture of infected neutrophils by dendritic cells in the skin inhibits the early anti-*Leishmania* response. PLoS Pathog. **8:**e1002536. http://dx.doi.org/10.1371/journal.ppat.1002536.
35. **Goncalves R, Zhang X, Cohen H, Debrabant A, Mosser DM.** 2011. Platelet activation attracts a subpopulation of effector monocytes to sites of *Leishmania major* infection. J. Exp. Med. **208:**1253–1265. http://dx.doi.org/10.1084/jem.20101751.
36. **Kimblin N, Peters N, Debrabant A, Secundino N, Egen J, Lawyer P, Fay MP, Kamhawi S, Sacks D.** 2008. Quantification of the infectious dose of *Leishmania major* transmitted to the skin by single sand flies. Proc. Natl. Acad. Sci. U. S. A. **105:**10125–10130. http://dx.doi.org/10.1073/pnas.0802331105.
37. **Sacks DL, Hieny S, Sher A.** 1985. Identification of cell surface carbohydrate and antigenic changes between noninfective and infective developmental stages of *Leishmania major* promastigotes. J. Immunol. **135:**564–569.
38. **Peters NC, Kimblin N, Secundino N, Kamhawi S, Lawyer P, Sacks DL.** 2009. Vector transmission of *Leishmania* abrogates vaccine-induced protective immunity. PLoS Pathog. **5:**e1000484. http://dx.doi.org/10.1371/journal.ppat.1000484.
39. **Ghosn EE, Cassado AA, Govoni GR, Fukuhara T, Yang Y, Monack DM, Bortoluci KR, Almeida SR, Herzenberg LA, Herzenberg LA.** 2010. Two physically, functionally, and developmentally distinct peritoneal macrophage subsets. Proc. Natl. Acad. Sci. U. S. A. **107:**2568–2573. http://dx.doi.org/10.1073/pnas.0915000107.
40. **Matzinger P, Kamala T.** 2011. Tissue-based class control: the other side of tolerance. Nat. Rev. Immunol. **11:**221–230. http://dx.doi.org/10.1038/nri2940.
41. **Constant SL, Brogdon JL, Piggott DA, Herrick CA, Visintin I, Ruddle NH, Bottomly K.** 2002. Resident lung antigen-presenting cells have the capacity to promote Th2 T cell differentiation in situ. J. Clin. Invest. **110:**1441–1448. http://dx.doi.org/10.1172/JCI16109.
42. **Peters NC, Hamilton DH, Bretscher PA.** 2005. Analysis of cytokine-producing Th cells from hen egg lysozyme-immunized mice reveals large numbers specific for "cryptic" peptides and different repertoires among different Th populations. Eur. J. Immunol. **35:**56–65. http://dx.doi.org/10.1002/eji.200425581.
43. **Gapin L, Bravo de Alba Y, Casrouge A, Cabaniols JP, Kourilsky P, Kanellopoulos J.** 1998. Antigen presentation by dendritic cells focuses T

cell responses against immunodominant peptides: studies in the hen egg-white lysozyme (HEL) model. J. Immunol. **160:**1555–1564.
44. **Bretscher PA, Wei G, Menon JN, Bielefeldt-Ohmann H.** 1992. Establishment of stable, cell-mediated immunity that makes "susceptible" mice resistant to *Leishmania major*. Science **257:**539–542. http://dx.doi.org/10.1126/science.1636090.
45. **Yamakami K, Akao S, Tadakuma T, Nitta Y, Miyazaki J, Yoshizawa N.** 2002. Administration of plasmids expressing interleukin-4 and interleukin-10 causes BALB/c mice to induce a T helper 2-type response despite the expected T helper 1-type response with a low-dose infection of *Leishmania major*. Immunology **105:**515–523. http://dx.doi.org/10.1046/j.1365-2567.2002.01394.x.
46. **Uzonna JE, Wei G, Yurkowski D, Bretscher P.** 2001. Immune elimination of *Leishmania major* in mice: implications for immune memory, vaccination, and reactivation disease. J. Immunol. **167:**6967–6974. http://dx.doi.org/10.4049/jimmunol.167.12.6967.
47. **Stamper LW, Patrick RL, Fay MP, Lawyer PG, Elnaiem DE, Secundino N, Debrabant A, Sacks DL, Peters NC.** 2011. Infection parameters in the sand fly vector that predict transmission of *Leishmania major*. PLoS Negl. Trop. Dis. **5:**e1288. http://dx.doi.org/10.1371/journal.pntd.0001288.
48. **Lira R, Doherty M, Modi G, Sacks D.** 2000. Evolution of lesion formation, parasitic load, immune response, and reservoir potential in C57BL/6 mice following high- and low-dose challenge with *Leishmania major*. Infect. Immun. **68:**5176–5182. http://dx.doi.org/10.1128/IAI.68.9.5176-5182.2000.